

A Solid State NMR Study of Dynamics in a Hydrated Salivary Peptide Adsorbed to Hydroxyapatite

Wendy J. Shaw,[‡] Joanna R. Long,[†] Allison A. Campbell,[§]
Patrick S. Stayton,^{*,†} and Gary P. Drobny^{*,‡}

Department of Bioengineering
Department of Chemistry
University of Washington, Seattle, Washington 98195
Pacific Northwest National Laboratory
Richland, Washington 99352

Received March 10, 2000
Revised Manuscript Received May 19, 2000

Proteins interact with biomineral surfaces to control crystal growth and final structure in biological systems ranging from seashell formation to teeth and bone.^{1,2} The elucidation of molecular recognition mechanisms at the organic–inorganic interface could provide inspiration for materials synthesis strategies. Solid-state NMR (SSNMR) has been shown to be a powerful tool for determining the secondary structure of surface adsorbed proteins,^{3–5} and can potentially provide important information on peptide dynamics at surfaces as a function of hydration.^{6,7} Both structure and dynamics have been associated with function in many biological systems^{8,9} so the dynamics of surface-bound proteins are likely an important aspect of peptide and protein function at biomineral surfaces.

Statherin is a small, multifunctional protein, which inhibits primary and secondary precipitation of hydroxyapatite (HAP) in saliva, as well as serving as a boundary lubricant.¹³ The acidic, N-terminal region of statherin binds strongly to HAP and inhibits HAP growth in situ. When adsorbed to HAP, the N-terminal 15 amino acid peptide of salivary statherin, SN15 (DpSpSEKFLRRIGRFG), exhibits a random coil structure at the pS₂pS₃ position near the N-terminus. The F₇L₈ region in the middle of the peptide exhibits a high degree of helical secondary structure and the C-terminal I₁₁G₁₂ position has also been observed to contain some helical structure.⁴ An investigation of peptide dynamics isotopically labeled at these positions in the SN15 peptide was conducted on hydrated samples to provide a correlation between structure and dynamics on the surface, which may provide insight into crystal engineering function. For this study, three separate peptides were synthesized with double isotopic backbone carbonyl carbon

labels at the following positions: pS₂pS₃, F₇L₈, and I₁₁G₁₂. Three additional peptides were synthesized containing single backbone carbonyl isotopic labels incorporated at the corresponding positions: pS₃, L₈, and G₁₂.

Dynamic information was obtained from cross polarization magic angle spinning (CPMAS) spectra by determining motionally averaged chemical shift tensor values¹⁰ for ¹³C-labeled backbone carbonyl carbons, which are very sensitive to molecular dynamics and electronic structure.¹¹ The principal elements of the CSA are designated σ_{11} , σ_{22} , and σ_{33} , with the isotropic chemical shift defined as $\sigma_0 = (1/3)(\sigma_{11} + \sigma_{22} + \sigma_{33})$. Particularly useful in comparing shielding tensors is the parameter $\Omega = |\sigma_{11} - \sigma_{33}|$, which describes the magnitude of the anisotropy.¹² Motions occurring at rates much larger than the CSA (i.e., $\gg 20$ kHz at a magnetic field of 11.75 T), effectively pre-average the CSA tensor. The principal elements of the motionally pre-averaged CSA tensor may be determined directly from the CPMAS spectrum and may be used to calculate dynamic amplitudes of motions occurring on time scales fast compared to the CSA.

In addition, relaxation measurements provide information on molecular motions. In particular, $T_{1\rho}$ measurements provide dynamic information on the time scale of 10^{-3} to 10^{-5} s,⁷ and thus extend to somewhat lower rates than those probed by pre-averaged CSA tensor elements. Although extracting correlation times from ¹³C $T_{1\rho}$ data is beyond the scope of this paper, comparison of ¹³C $T_{1\rho}$ values for specific sites under different sample conditions provides a qualitative determination of millisecond-scale dynamics.

Figure 1 shows CPMAS spectra of the SN15 peptide bound to hydroxyapatite at the six labeled positions. On the left, spectra for the hydrated samples clearly show that motional averaging on the order of the chemical shift anisotropy increases as the probe site is moved away from the N-terminus and toward the C-terminus. On the right, CPMAS spectra of the lyophilized samples collected with identical instrumental parameters show typical CSA values for rigid carbonyl carbons in a peptide bond with an anisotropy approaching 150 ppm.⁶ The results for both lyophilized and hydrated surface adsorbed samples, along with results for the peptide lyophilized from buffered solution, are summarized in Table 1. With hydration, there is little change in the backbone carbonyl carbon CSA at the phosphoserine positions, with anisotropies narrowing by only 6 and 8 ppm, respectively. Slightly more change is observed at the phenylalanine and leucine positions where Ω narrows by 10 and 28 ppm, respectively. The most remarkable motional averaging is observed at the isoleucine ($\Delta\Omega = 75$ ppm) and glycine ($\Delta\Omega = 91$ ppm) positions. The hydrated spectra shown here visibly demonstrate the rigidity of the phosphoserine residues, with increasing motion until the presence of large amplitude motion with frequency on the order or greater than 10^{-5} s is observed at the I₁₁ and G₁₂ positions.

To further investigate the dynamics, ¹³C $T_{1\rho}$ measurements were obtained at a radio frequency field of 42 kHz for each of the doubly labeled peptides. The ¹³C $T_{1\rho}$ values for the peptides lyophilized from buffer and for lyophilized surface-adsorbed samples were greater than 25 ms in all cases, consistent with little motion on the kilohertz time scale. The hydrated surface adsorbed samples had ¹³C $T_{1\rho}$ values > 25 , 11, and 3 ms for pS₂pS₃, F₇L₈, and I₁₁G₁₂, respectively. The significantly shorter $T_{1\rho}$ values in the middle and at the C-terminus for the hydrated surface adsorbed samples correlate well with the observed spectra and are consistent with increased motion at a frequency greater than 10^3 Hz.

A peptide–HAP interaction model that is consistent with the current dynamic studies and previous structural studies is shown in Figure 2. The acidic N-terminus plays a key role in the binding of salivary statherin, with strong interactions between the HAP and the phosphorylated serines and the aspartic/glutamic acid side

* Address correspondence to this author.

[‡] Department of Chemistry, University of Washington.

[†] Department of Bioengineering, University of Washington.

[§] Pacific Northwest National Laboratory.

- (1) Hunter, G. K. *Curr. Opin. Solid State Mater. Sci.* **1996**, *1*, 430–435.
- (2) Weiner, S.; Addadi, L. *J. Mater. Chem.* **1997**, *7*, 689–702.
- (3) Long, J. R.; Dindot, J. L.; Zebroski, H.; Kiihne, S.; Clark, R. H.; Campbell, A. A.; Stayton, P. S.; Drobny, G. P. *Proc. Natl. Acad. Sci.* **1998**, *95*, 12083–12087.
- (4) Shaw, W.; Long, J.; Dindot, J.; Campbell, A.; Stayton, P.; Drobny, G. *J. Am. Chem. Soc.* **2000**, *122*, 1709–1716.
- (5) Fernandez, V. L.; Reimer, J. A.; Denn, M. M. *J. Am. Chem. Soc.* **1992**, *114*, 9634–9642.
- (6) Gu, Z.; McDermott, A. *J. Am. Chem. Soc.* **1993**, *115*, 4282–4285.
- (7) Schaefer, J.; Stejskal, E. O.; Buchdahl, R. *Macromolecules* **1977**, *10*, 384–405.
- (8) Gehegin, K.; Meints, G. A.; Hatcher, M. E.; Drobny, G. P. *Biochemistry* **2000**, *39*, 4939–4946.
- (9) Hatcher, M. E.; Mattiello, D. L.; Meints, G. A.; Orban, J.; Drobny, G. P. *J. Am. Chem. Soc.* **1998**, *120*, 9850–9862.
- (10) Herzfeld, J.; Berger, A. E. *J. Phys. Chem.* **1980**, *73*, 6021–6030.
- (11) Ruocco, J. J.; Siminovitch, D. J.; Long, J. R.; Das Gupta, S. K.; Griffen, R. G. *Biophys. J.* **1996**, *71*, 1776–1788.
- (12) Spiess, H. W. *Rotation of Molecules and Nuclear Spin Relaxation*; Springer: Berlin, 1978; Vol. 15.
- (13) Raj, P. A.; Johnsson, M.; Levine, M. J.; Nancollas, G. H. *J. Biol. Chem.* **1992**, *267*, 5968–5976.

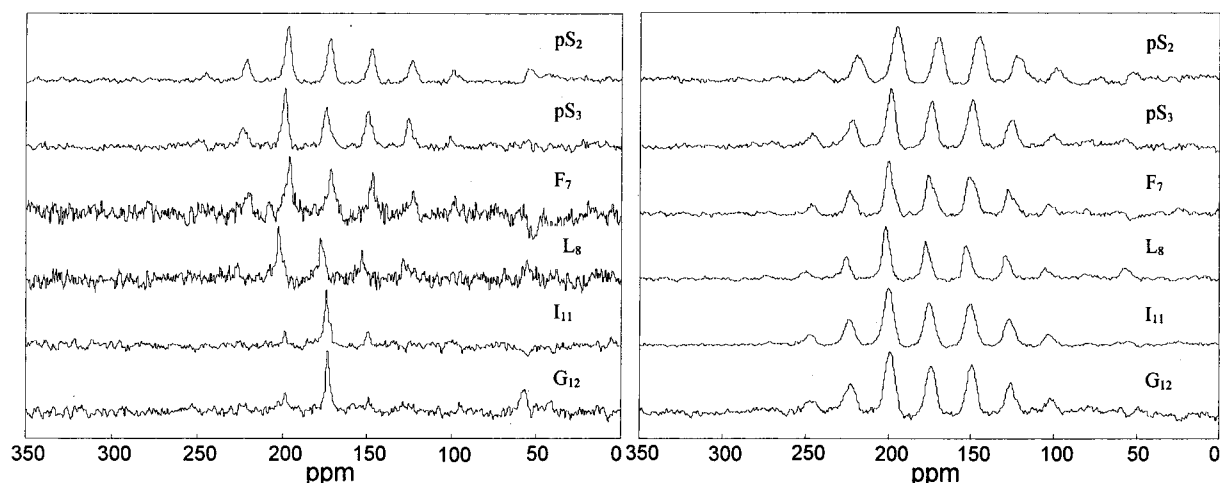


Figure 1. ^{13}C CPMAS spectra of SN15 peptides adsorbed to HAP: left, hydrated and right, lyophilized, with the site of ^{13}C enrichment indicated. Samples were prepared by adsorbing 2 mM peptide in modified PBS (100 mM NaCl, 40 mM KCl, 4.3 mM Na_2HPO_4 , 1.4 mM KH_2PO_4) to hydroxyapatite crystals (prepared in our labs, with a surface area of $77\text{ m}^2/\text{g}$) for 4 h followed by repeated washes with buffer. The resulting slurry was then transferred to a rotor, leaving the final surface adsorbed peptide in the bulk hydrated state. To facilitate direct comparisons between hydrated and lyophilized samples, the hydrated spectra were obtained first. The samples were then frozen and lyophilized in the rotor prior to acquisition of the lyophilized spectra. Each spectrum consists of 10 000 scans taken on a spectrometer operating at a 125.74 MHz ^{13}C frequency with a 3 kHz sample spinning rate. Subtracting the single isotopically labeled spectra from the doubly labeled spectra resulted in the three spectra for SN15-S₂, SN15-F₇, and SN15-I₁₁, and each sample was corrected for natural abundance signal. The lower apparent signal-to-noise for the F₇ and L₈ positions is a result of dissimilar amounts of peptide adsorbing on the surface, resulting in lower signal-to-noise for the SN15-L₈ spectrum, and upon subtraction from SN15-F₇L₈ and lower S/N for the SN15-F₇ spectrum.

Table 1. Anisotropy (in ppm) as a Function of Position in the Peptide and Sample Preparation, as Indicated

	pS ₂	pS ₃	F ₇	L ₈	I ₁₁	G ₁₂
lyophilized	146	148	147	150	141	148
bound, lyophilized	145	148	144	144	144	148
bound, hydrated	137	141	134	116	70	57

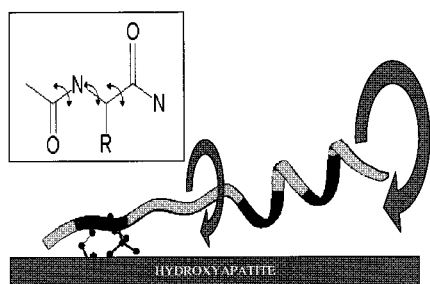


Figure 2. A schematic of the proposed interaction between the N15 peptide and the surface. Darkened regions correspond to labeled residues, with arrows indicating one possible collective motion, and the inset indicate the torsional contributions. The number of degrees of freedom available to the C-terminal residues supports a multiaxial, large frequency and amplitude motion.

chains. In the SN15 peptide, the random coil conformation in this region could allow most of these acidic groups to directly interact with the HAP surface, leading to tight interactions and the rigid dynamics observed in this region. The α -helical middle region of the peptide displayed increased dynamics and is thus less rigidly interacting with the surface, while the C-terminal end of the peptide must have very little interaction with the surface. The averaging of the motion at the I₁₁ and G₁₂ positions is most consistent with a multiaxial, rather than uniaxial motion. Two reasonable interpretations would be the following: (1) the occurrence of large-amplitude librations of the peptide backbone at high frequency (relative to the CSA) which are localized to

the immediate environments of the spin labels or (2) a combination of librations about a number of axes from many different positions along the peptide backbone. The experiments performed here do not address the orientation of the helix to the surface, and thus the current results do not uniquely determine a detailed dynamic motional model.

There are several functional roles that the observed mobility of statherin may play. It has been observed that even at low coverage, statherin is found to inhibit secondary precipitation of calcium phosphates approximately 2 times more than expected, based on the calculated coverage.^{14,15} With large amplitude mobility, a larger surface area is effectively covered than that predicted for a rigid protein, allowing increased crystal growth inhibition. The dynamic behavior of the C-terminal portion of SN15 may also contribute to the lubricity of the protein, while the rigidly attached N-terminus serves to prevent detachment during mastication.

To more specifically constrain and determine the motional modes, we are currently determining the orientation of the peptide and full statherin on the surface, along with further relaxation measurements.

Acknowledgment. The authors would like to thank Nathan Oyler for providing simulation code and Rob Britschgi for peptide purification. Support from the Department of Energy through Associated Western Universities (W.J.S.), National Dental Institute Grant DE 12554-01, and the National Science Foundation Grant DMR-9616212 is gratefully acknowledged.

Supporting Information Available: Chemical shift tensor values and σ and η parameters are tabulated and the preparation and characterization of hydroxyapatite is also presented (PDF). This material is available free of charge via the Internet at <http://pubs.acs.org>.

JA000878Q

(14) Moreno, E. C.; Varughese, K.; Hay, D. I. *Calcif. Tissue Int.* **1979**, *28*, 7–16.

(15) Hay, D. I.; Smith, D. J.; Schluckebier, S. K.; Moreno, E. C. *J. Dent. Res.* **1984**, *63*, 857–863.